Applied Energy 279 (2020) 115872

Contents lists available at ScienceDirect

Applied Energy

journal homepage: www.elsevier.com/locate/apenergy

Effective non-intrusive load monitoring of buildings based on a novel multi-descriptor fusion with dimensionality reduction

Yassine Himeur [a,*], Abdullah Alsalemi [a], Faycal Bensaali [a], Abbes Amira [b]

[a] Department of Electrical Engineering, Qatar University, Doha, Qatar
[b] Institute of Artificial Intelligence, De Montfort University, Leicester, United Kingdom

ARTICLE INFO

Keywords:
Non-intrusive load monitoring
Energy efficiency
Feature extraction
Fusion of time-domain descriptors
Dimensionality reduction
Bagging decision tree

ABSTRACT

Recently, a growing interest has been dedicated towards developing and implementing low-cost energy efficiency solutions in buildings. Accordingly, non-intrusive load monitoring has been investigated in various academic and industrial projects for capturing device-specific consumption footprints without any additional hardware installation. However, its performance should be improved further to enable an accurate appliance identification from the aggregated load. This paper presents an efficient non-intrusive load monitoring framework that consists of the following main components: (i) a novel fusion of multiple time-domain features is proposed to extract appliance fingerprints; (ii) a dimensionality reduction scheme is introduced to be applied to the fused time-domain features, which relies on fuzzy-neighbors preserving analysis based QR-decomposition. The latter can not only reduce feature dimensionality, but it can also effectively decrease the intra-class distances and increase the extra-class distances of appliance features; and (iii) a powerful decision bagging tree classifier is implemented to accurately classify electrical devices using the reduced features. Empirical evaluations performed on three real datasets, namely ACS-F2, REDD and WHITED collected at different sampling rates have shown a promising performance, according to the accuracy and F1 score achieved using the proposed non-intrusive load monitoring system. Reported accuracy and F1 score have reached both 100% for the WHITED dataset, 99.79% and 99.76% for the REDD dataset, and up to 99.41% and 98.93% for the ACS-f2 dataset, respectively. The outstanding performance achieved using the proposed solution determines its effectiveness in collecting individual-appliance consumption data and in promoting energy saving behaviors.

1. Introduction

Building sector represents a major energy consumer, which actively participates in the extensive and increasing energy demands. It is in charge of up to 39% of all greenhouse gases and carbon emissions. This percentage could be increased in regions having extreme dry, subtropical desert climates, as the case in the middle east, in which buildings could be responsible of consuming up to 70% of the produced energy [1]. From another side, monitoring energy consumption in the buildings is of utmost importance to promote energy efficiency and reduce carbon emissions. It is part of the smart grid field, which is a hot applied energy topic, where recent trends in artificial intelligence, Internet of things (IoT) and feature extraction play a major role in developing low-cost solutions using existed power grids [2].

In this context, smart grids have received a great attention in recent years due to their promising effectiveness in saving energy and reducing carbon emission [3,4]. The use smart-meters with the development of powerful and intelligent algorithms to monitor energy consumption and collect statistics are the core of the smart grid technology [5]. Consequently, enormous efforts are presently being put in place to increase the energy efficiency of domestic and commercial infrastructures using the knowledge of power grids [6,7]. Recent works have demonstrated that residential and public buildings are responsible for more than 40% of global electricity usage, in which 20% can be preserved through adopting the knowledge of smart grids [8,9].

In addition, using new technologies such as smartphones and smart meters for load monitoring and behavioral change can assist end-users to build a better energy consumption profile. This is possible by triggering personalized recommendations at the right-moment at an appliance-level and addressing them to the end-user [10,11]. However, even if the extensive use of smart meters can help picking up specific energy consumption footprints at a household, the cost of such installation is prohibitive and it is combined with hardware equipment and

* Corresponding author.
E-mail addresses: yassine.himeur@qu.edu.qa (Y. Himeur), a.alsalemi@qu.edu.qa (A. Alsalemi), f.bensaali@qu.edu.qa (F. Bensaali), abbes.amira@dmu.ac.uk (A. Amira).

https://doi.org/10.1016/j.apenergy.2020.115872
Received 23 May 2020; Received in revised form 31 August 2020; Accepted 12 September 2020
Available online 17 September 2020

enormous effort [12,13]. Non-intrusive load monitoring (NILM) is a strong alternative for designing a powerful, precise and scalable load monitoring in residential sector that is easy to deploy with no extra cost. In addition, the gains of NILM can not be limited to only end-users, but it can also contribute in enhancing operational efficiency, helping providers to minimize operational costs, and improving public health and well-being [14,15].

Developing an efficient NILM system requires making use of a feature extraction module that can capture the particular consumption fingerprint of each electrical device along with a powerful classifier [16,17]. The feature extraction process can hence help in reducing the distances between appliances pertaining to the same class [18]. Building such a feature descriptor is hard to achieve since the power consumption signal has various characteristics that should be considered [19,20]. To that end, the fusion of multiple descriptors is among the ambitious solutions that help in developing an efficient descriptor owing to the fact that it combines different properties of various descriptor features and thus leading to a better feature representation, which improves the accuracy and F1 score of the classification.

Moving forward, identifying appliances connected to the smart grid at a high accuracy is of utmost importance in order to provide end-users with accurate appliance-level consumption footprints, and hence helping them in correctly analyzing and adjusting their consumption behaviors. To that end, in this paper, an effective NILM procedure is proposed to address the above-mentioned challenges and offer precise device-specific consumption data to end-users, in which 100% accuracy and 100% F1 score have been attained on worldwide household and industry transient energy dataset (WHITED), 99.79% accuracy and 99.76% F1 score have been achieved under reference energy disaggregation dataset (REDD), and up to 99.41% accuracy and 98.93% F1 score have been reached under appliance consumption signatures version 2 (ACS-f2) dataset. Overall, the main contributions of this framework can be summarized as follows:

- A simple yet effective multi-descriptor fusion is proposed, which provides a high device recognition performance using the joint-use of various time-domain (TD) descriptors. Accordingly, the proposed fusion of time-domain features, namely FTDF, fuses features of various descriptors generated from the current window and those collected from previous windows for a more efficient appliance recognition. In this respect, the regional variation of the power consumption properties is correlated to the semi-global variation as drawn off using the TD analysis of the past windows.
- A dimensionality reduction technique named fuzzy-neighbors preserving analysis (FNPA) based QR-decomposition (FNPA-QR) is applied to the FTDF feature vectors derived in the first stage. The FNPA-QR has the particularity of being able to decrease the intra-class distances and increase the extra-class distances of the appliance features.
- A decision bagging tree (DBT) classifier is implemented aiming at effectively classifying the electrical devices using the FTDF based FNPA-QR features.
- A brief hierarchical taxonomy with a comprehensive overview of recent strategies based on appliance features is provided as well.
- The proposed NILM framework is validated on three realistic power consumption databases, namely the REDD, ACS-F2 and WHITED having different sampling frequencies to check its robustness in different scenarios. Furthermore a comprehensive comparison is carried out versus recent NILM systems on the REDD dataset. In addition, the proposed solution is experimentally validated under different computing devices to prove its application in real-world scenarios.

The paper is organized as follows. In Section 2, we provide a comprehensive overview of NILM systems based on a feature-based taxonomy. In Section 3, the different modules of the proposed NILM architecture are presented in detail. In Section 4, the numerical results of the proposed NILM solution are assessed and compared to recent NILM approaches. Moreover, the proposed solution is validated experimentally using different computing devices. Finally, the findings of this work are summarized in Section 5 and future directions are discussed as well.

2. Related works

2.1. Feature based taxonomy

Appliance feature extraction plays a prominent role towards inferring the energy consumption footprints of each device. This step is responsible for extracting a fine-grained and unique signature of each appliance from its power consumption data. Therefore, the extracted features help in identifying particular properties of each device, which thus can be employed for classification and identification [21,22]. Generally, appliance fingerprints correspond to measurable parameters that supply appliance-specific data drawn from physical measures. Three main categories of non-intrusive appliance features can be found in the state-of-the-art: steady-state fingerprints, transient-state signatures and non-conventional characteristics. A hierarchical categorization is performed in Fig. 1 to summarize the appliance feature types used for NILM process.

2.1.1. Steady state features

Steady-state patterns include characteristics derived from electrical devices, particularly at their stationary periods (i.e. there are no transitions between two states), which means they are working at a regular electricity usage level. Most importantly, a steady-state fingerprint represents properties picked up during the analysis performed between two consecutive and operative steady-states. This kind of feature is most probably related to the change in power usage and voltage–current (V–I) trajectory. Typically, this type of characteristics can be categorized into four sub-groups as follows:

- Power change analysis: techniques belonging to this category are mainly focusing on collecting real and reactive power with a view of providing the most distinguishing characteristics of each device [23]. To capture such properties, the power usage level is estimated at a specific time sampling rate [24,25].
- Time–frequency analysis: it has been widely adopted in various energy applications, in which feature extraction is required. It helps in capturing pertinent power features by analyzing their time–frequency presentations. Specifically, in the context of NILM, it has been deployed to overcome overlapping issues and provide fine-grained representations of power consumption signals [20,26]. Various time–frequency descriptors have been used to implement NILM systems, among them the wavelet transform [27], multi-scale wavelet packet tree [28], S-transform [29] and spatio-temporal pattern network [30].
- V-I trajectory features: a set of pertinent characteristics is derived from the waveform of the V-I trajectory. This form portrays relevant properties, among others, the asymmetry [31,32], wave-shape representation [33,34], slope change and enclosed area [31].
- Harmonic features: these methods focus on studying harmonics of electrical appliances currents using a frequency analysis [35,36]. In addition, they can generate supplementary data on appliances' properties and hence help in improving the classification performance [37].

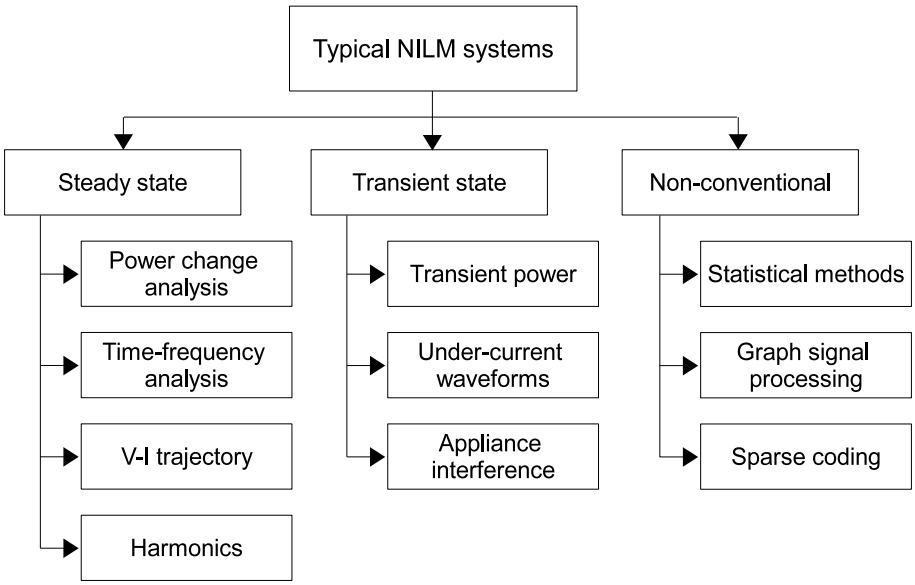

Fig. 1. Hierarchical categorization of NILM systems based on feature extraction schemes.

2.1.2. Transient state features

In some scenarios, two different devices can have similar energy consumption records and hence reducing the discrimination ability of classifiers to identify either appliance. In this regard, analyzing the transient states, i.e. the consumption scenario of a device when shifting from a steady state to another one can produce crucial data. We can find the following sub-categories:

- Transient power: transient power data are collected to represent each device. In [20,38], a transient event-detection approach is proposed for determining the operating schedule, finding properties of the physical behaviors of the loads connected to the electrical network and thereby modeling the electrical appliances.
- Under-current waveforms: this kind of features is used together with other characteristics to model device signatures [39,40].
- Interference features: interferences generated by the domestic devices connected to the electrical wires can also be used as unique fingerprints to identify the appliances [41].

2.1.3. Non conventional features

The third group of appliance characteristics is denoted as non-conventional, since this class incorporates all features that do not pertain to the groups mentioned previously. This category of features can be also decomposed to the following sub-classes:

- Statistical features: this type of feature focuses mainly on collecting statistical parameters and further using statistical models to represent appliances footprints [42]. NILM systems relying on the use of statistical features are called non-event based detection techniques since they deploy statistical models to separate the main loads into appliance-specific fingerprints, such as hidden Markov models (HMMs) [43,44], probabilistic models [45], higher-order statistics (HOS) [46] and factorial HMMs [25,40].
- Graph signal processing (GSP) features: they aim at representing the stochastic properties of signals using graphs [47]. In fact, GSP is a hot research topic relies on the fact that power signals can be represented with generic data representation forms via the use of graphs. This leads in a better description of geometric structures of power signals [48,49]. Different NILM frameworks have been proposed based on graph-based filtering [50], graph shift quadratic form constraint [51] and graph-based event detection [52].
- Sparse coding features: in this case, the energy disaggregation framework is treated as a blind source separation problem and recent sparse coding schemes are then applied to split an aggregated power consumption signal into the specific appliance based profiles [53]. Various NILM systems are recently proposed based on deep sparse coding [54], Bayesian discriminative sparse coding [55] and modeling appliance perturbations as sparse errors [56].

2.2. Discussion

Although the traditional NILM techniques based on steady-state and transient-state features have been widely studied in the state-of-the-art, they still experience various limitations and imperfections. For example, (i) most of them have modest appliance recognition performance, (ii) capturing transient states can limit their detection accuracy if multiple appliances are turning on/off simultaneously, and (iii) Although their performance could be enhanced using deep learning as demonstrated in [57], however, this makes their implementation on embedded systems hard because of the complexity of deep neutral networks. For non conventional NILM schemes, because they depend on resolving complex probabilistic and stochastic models, their implementation on embedded platforms is not straightforward, even very hard to achieve. Further, their performances are still less than state-of-the-art and more investigation is required to improve them. Moreover, most of the existing NILM systems are validated only on one dataset, which cannot prove their efficiency on other datasets with distinct sampling frequencies.

However, in this framework, we propose an NILM system that can achieve high performance in identifying appliances. Specifically, the proposed solution is built using a simple yet effective fusion of TD features, an improved dimensionality reduction and a powerful DBT classifier. This makes the proposed solution very effective in discriminating between appliances from distinct appliance classes and on the flip side has a good capability to reduce the distance between appliances from the same category. Moreover, the proposed NILM system has been validated on three different datasets with distinct sampling frequency. Therefore, the proposed approach provides a set of benefits that can be summarized as follows:

- Power consumption footprints in ACS-F2 [58] and WHITED [59] datasets have been gathered from a large number of devices from

distinct manufacturers (i.e. every device category encompasses several devices from distinct brands). This enables the evaluation of the proposed NILM system to identify a specific appliance type even if the former is trained using data of other appliances pertaining to the same class but from different manufacturers (brands). Therefore, this helps in using our system for an unseen house without the need to train it again since the probability of having a new appliance that does not pertain to any appliance classes used in the training step is very low. Moreover, this proves also that there is no need to apply a transfer learning as it is the case with other deep learning based solutions.

- While under REDD dataset [60], energy consumption footprints have been gleaned from the same households' appliances, but for different days, in which each daily power consumption collected from a specific appliance represents a new signature that can help in its identification. Therefore, this proves that the end-user can train the proposed NILM system using its own data (i.e. daily power consumption could be collected and then used to train our system).
- Both evaluation scenarios considered in this framework demonstrate that the proposed NILM system can be generalized to an unseen house or can also use the data of the end-user in the training process. In this context, the evaluation studies conducted in this paper help in consolidating the credibility of the propose work.
- Furthermore, the use of DBT in our solution has been selected since this kind of classifiers does not require a large amount of data in the training step in comparison with other models, such as deep neural networks (DNN), convolutional neural networks (CNN) and generative adversarial networks (GAN). The latter require large-scale datasets and hence their application for non-intrusive load monitoring is not practical. While, for our solution, it is possible to train the DBT classifier with much less data that can easily be collected in a household.

3. Proposed system

After gathering power consumption profiles from the aggregated circuit using a central sub-meter in a household, the NILM system can afterward capture the consumption fingerprint of each device connected to the whole circuit. Accordingly, in the proposed solution, an NILM architecture is implemented through the following main steps, as indicated in Fig. 2.

3.1. Data collection and pre-processing

With reference to the data collection process, three major properties can affect the NILM platform and they are summarized as follows: (i) the nature of power that can be active or reactive; (ii) energy consumption resolution that can be translated as the lower power level that can be captured by the collection platform; and (iii) the sampling frequency that constitutes two main groups: the low-frequency and high frequency. The first class refers to sampling frequencies up to 1 kHz while the second group includes sampling rates above 1 kHz [61].

In other words, data acquisition and pre-processing phases refer to the manner the power signals are gathered, the hardware implementation to capture data and also the process used to handle raw data. In this direction, it is required to clean the data by checking for missing observations and thus replacing them by null values. In addition, either an upsampling or downsampling process can be applied to the collected data as well as required by the developed application. In our case, we use three realistic databases, namely, the ACS-F2, REDD and WHITED, they were gathered at 0.1 Hz, 0.33 Hz and 44 kHz, respectively.

3.2. Energy disaggregation

The major concern of energy disaggregation relies on splitting the whole power signal into various fine-grained elements. In a household, the outputs are the specific load usage profiles of every distinct device. Therefore, the aim is to recognize each device and detect how much energy it consumes. The power aggregation p_A of N appliances in a time interval T, is given as:

$$p_A(t) = p_n(t) + \sum_{i=1}^{N} p_i(t), \quad t \in \{1, T\} \tag{1}$$

with p_i represents the power of the device i and p_n depicts the power of noise generated by the electric interferences.

However, in order to split the aggregated power signal into fine-grained elements, an event detection step should be performed. Since the primary objective of this paper relies on designing a novel feature extraction descriptor and dimensionality reduction strategy using a powerful classifier to identify appliances, in the event detection stage we just use the edge detector module [62] implemented in the NILMTK platform [63] to extract power events, from which the relevant features will then be extracted.

To extract power events, the aggregated power signal is fed into an edge detector, namely a transient-passing step change detector, which is based on estimating the first derivative of power signals. Thus, it captures the times and lengths of all steplike changes. In this regard, an edge detection using first derivative has been applied to the aggregated appliance power signal p_A to extract its power event e, as follows:

$$e = \text{abs}\left(\frac{dp_A}{dt}\right) \cong \text{abs}\left(\lim_{\Delta t \to 0} \frac{p_A(t+\Delta t) - p_A(t-\Delta t)}{\Delta t}\right) \tag{2}$$

where $\Delta t = 1$ is used in our case and abs refers to the absolute operator.

Specifically, this detector divides the aggregated power signals into two kinds of periods, defined as steady power and transient power. Following, the variations between the steady states and transient period help to define the step-changed length. Accordingly, the time of the first observation in every transient period and its associated magnitude gives a time-stamp to separate between power events pertaining to different appliances. The whole power event vector is represented as $e = [e^1, e^2, \ldots, e^N]$ and each e^i $(i = 1, 2, \ldots, N)$ refers to the event vector representing the individual appliance i.

3.3. Feature extraction

After detecting the power events using the edge detector in NILMTKL [62,63], the feature extraction techniques are then applied to each power event vector separately to derive the appliance based signatures.

3.3.1. Time-domain (TD) descriptors

With the view of describing the TD feature descriptors used under our framework, the detected power event vector of each ith individual appliance, denominated as: $e^i(j)$, where $j = 1, 2, \ldots, \zeta$ and ζ refers to the length of the power event vector, is fed into the feature extraction module with the intention of deriving their TD peculiarities. A windowing process is applied to each power event vector e^i, where a window length V is utilized and the TD property $P(k)$ of each window k ($k = 1, 2, \ldots, K$ and K represents the whole number of extracted windows) is then collected as follows:

- Root mean square feature (RMSF) [64]

$$P_{F1}(k) = P_{RMSF}(k) = \sum_{j=1}^{V} \sqrt{\frac{1}{V}(e_j^i)^2} \tag{3}$$

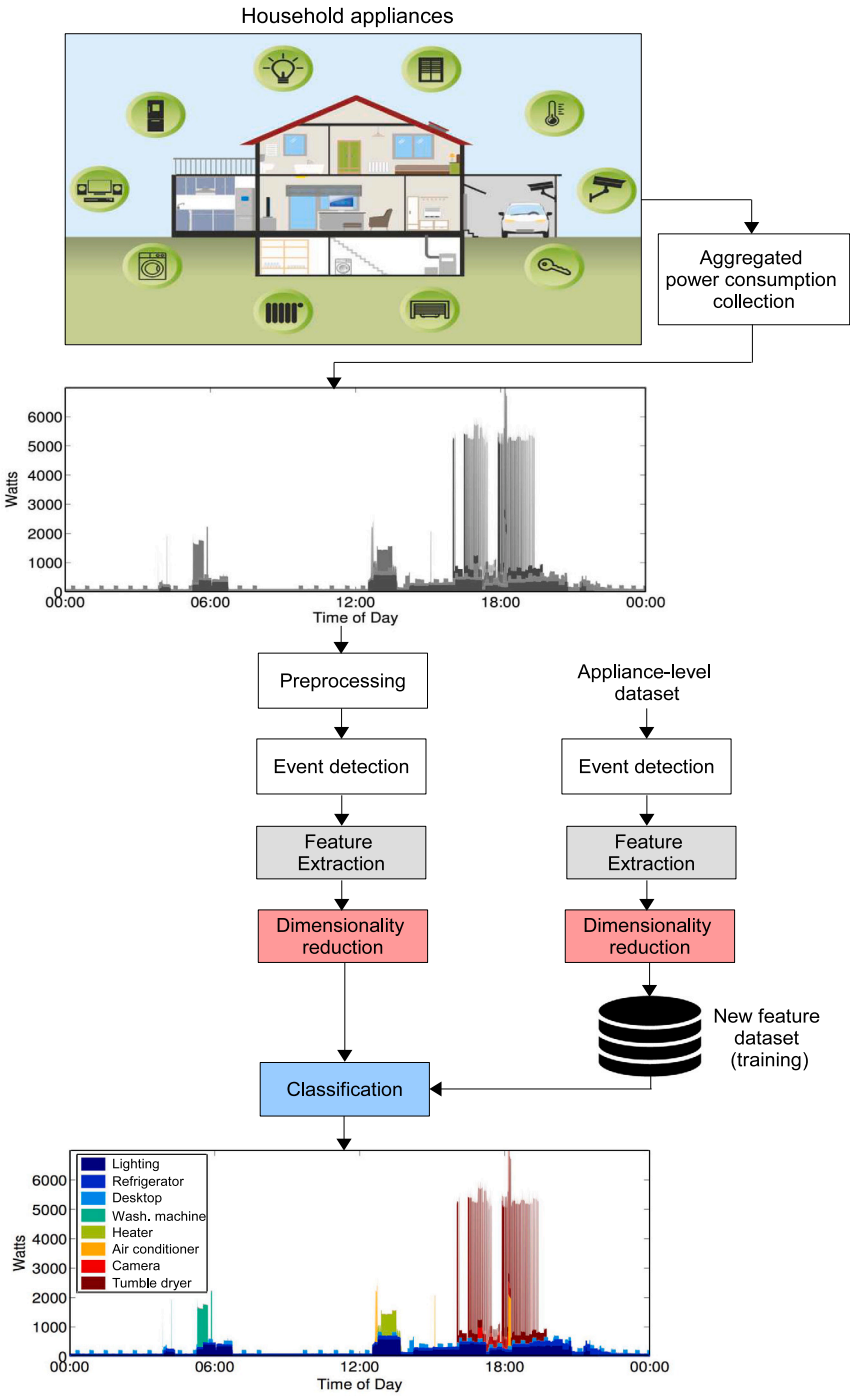

Fig. 2. Block diagram of the proposed NILM system.

- Mean absolute deviation feature (MADF) [65]

$$P_{F2}(k) = P_{MADF}(k) = \sum_{j=1}^{V} \frac{1}{V} \left| e_j^i - \mu \right| \tag{4}$$

where μ represent the central tendency,

- Integrated absolute magnitude feature (IAMF) [65]

$$P_{F3}(k) = S_{IAMF}(k) = \frac{1}{V} \sum_{j=1}^{V} \frac{(e_j^i)^2}{2} \mathrm{sgn}(e_j^i) + \mu \tag{5}$$

- Waveform length feature (WLF) [64]

$$P_{F4} = P_{WLF} = \log\left(\sum_{j=1}^{V-1} \left| e_{j+1}^i - e_j^i \right| \right) = \log\left(\sum_{j=1}^{V-1} \left| \Delta e_j^i \right| \right) \tag{6}$$

- Zero crossing feature (ZCF) [66]

$$P_{F5}(k) = P_{ZCF}(k) = \sum_{j=2}^{V} \left| \mathrm{sgn}(e_j^i) - \mathrm{sgn}(e_{j-1}^i) \right| \tag{7}$$

- Slope sign change feature (SSCF) [67]

$$P_{F6}(k) = P_{SSCF}(k) = \sum_{j=2}^{V-1} f[(e_j^i - e_{j-1}^i) \times (e_j^i - e_{j+1}^i)] \tag{8}$$

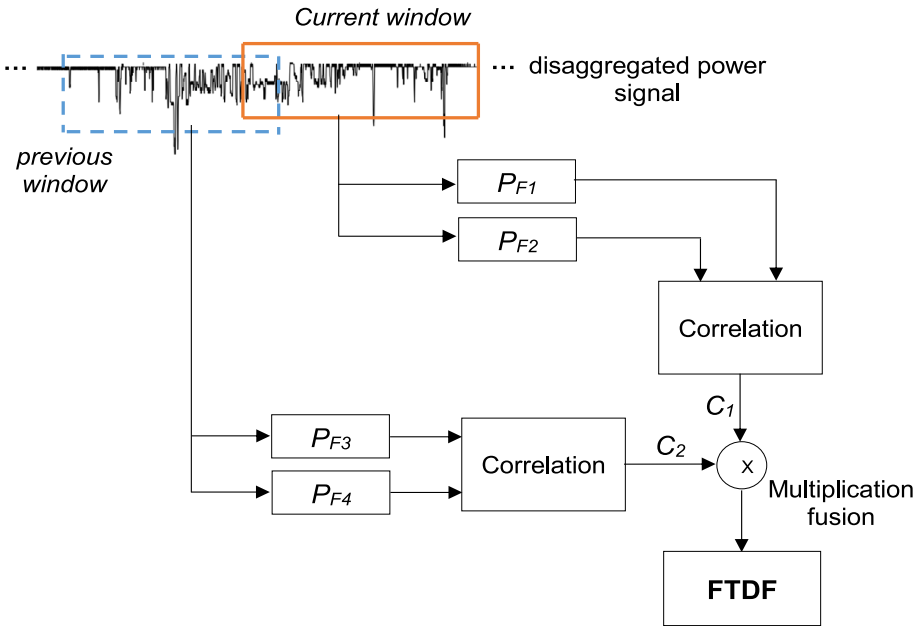

Fig. 3. Block diagram of the proposed fusion of TD features (FTDF) scheme.

where

$$f(e^i) = \begin{cases} 1 & \text{if } e^i \geq \text{threshold} \\ 0 & \text{otherwise} \end{cases} \quad (9)$$

- Auto-regressive feature (ARF) [67]

$$P_{F7}(k) = P_{ARF}(k) = \sum_{j=1}^{V} \left(\sum_{a=1}^{A} b_a e^i_{j-a} + w_j \right) \quad (10)$$

where e^i_{j-a} are the previous samples of the power consumption signal, w_j is a white noise and A represents the auto-regressive (AR) model order and b the weights. Under this framework $A = 15$ is considered.

After extracting the power features $P(k)$ from different sliding windows using an overlapping process, these data are concatenated to form the whole feature vector of the power consumption signal $P_F = [P(1), P(2), \ldots, P(K)]$.

It is worth noting that the first five TD descriptors, P_{F1}–P_{F5} have the advantage of being simple and fast to execute. Further, the four first descriptors P_{F1}–P_{F4} usually have good performance in extracting pertinent feature as it will be demonstrated through this framework. For the P_{F6} and P_{F7} descriptors, they have the characteristic of being more complex in comparison to the other descriptors although they provide moderate performance.

The aforementioned descriptors have been selected in this study to extract the features of appliance power signals because they are well-known descriptors used to extract TD features. In addition, they present a low time complexity in comparison with other frequency-domain of time-scale descriptors. They have been widely used to extract the pertinent characteristics of other types of signals such as electrocardiogram (ECG), electroencephalogram (EEG) [64], Myoelectric [65]. Moreover, their performance can be more improved if a fusion strategy is considered since these descriptors will complement each other to design an efficient descriptor.

3.3.2. Fusion of TD features (FTDF)

In this section, a data fusion strategy named FTDF is developed using the outputs of four TD descriptors from those described in the previous section. To describe the estimation of the final fusion vector, we take the example of the first four descriptors P_{F1}, P_{F2}, P_{F3} and P_{F4}. We proceed in the same manner if the other descriptors are selected, i.e. P_{F5}, P_{F6} and P_{F7}. First, for each disaggregated signal e^i, the selected descriptors are grouped into two couples, in which each couple includes two different feature descriptions that are extracted using two distinct descriptors. Following, these two couples are applied on two different, overlapping windows (the first couple of descriptors is applied to the current window while the second one is applied to its previous, overlapping window). Moving forward, the cross-correlation is measured between each couple. In theory, the cross-correlation between two TD vectors P_{F1} and P_{F2} is defined as:

$$R^i_{P_{F1}P_{F2}} = E\{P_{F1}(u+m)P^*_{F2}(u)\} = E\{P_{F1}(u)P^*_{F2}(u-m)\} \quad (11)$$

where $-\infty < u < \infty$, $()^*$ represents the complex conjugation, and E is the expected value operator. In practice, $u = 1, 2, \ldots, U$, in which U represents the length of P_{F1} and P_{F2} and $m = 1, 2, \ldots, 2\times U - 1$, therefore the relative cross-correlation $\hat{R}$ is estimated as follows:

$$\hat{R}^i_{P_{F1}P_{F2}}(m) = \begin{cases} \sum_{u=0}^{U-m-1} P_{F1}(u+m)P_{F2}(u) & m \geq 0 \\ R^i_{P_{F2}P_{F1}}(-m) & m < 0 \end{cases} \quad (12)$$

Next, the generated output correlation C_1 is given as:

$$C^i_1(m) = \hat{R}^i_{P_{F1}P_{F2}}(m - U), \quad m = 1, 2, \ldots, 2U - 1 \quad (13)$$

We then proceed with the same manner to estimate C_2 the correlation between P_{F3} and P_{F4}. Finally, a multiplication fusion is applied using the obtained correlation vectors C^i_1 and C^i_2, which is defined as

$$C^i = C^i_1 \times C^i_2 \quad (14)$$

where $\times$ is the multiplication operator.

The flowchart of the proposed FTDF approach is depicted in Fig. 3, where the variation of the power signal at each window is obtained using two different, overlapping windows. Explicitly, the correlation from the current window obtained using two different descriptors is fused with the correlation generated from the previous overlapping window using two other descriptors, and so forth.

3.4. Dimensionality reduction using FNPA-QR

After extracting the TD features, the dimensionality reduction based on FNPA-QR is applied, which is a variant of fuzzy-linear discriminant

Algorithm 1: The FNPA-QR algorithm used to represent the feature vectors in the new feature projection space.

Result: Y_i': the reduced version of the feature vector Y_i

a. Consider Y_i to be as the feature vector C^i obtained using the FTDF to represent a specific disaggregated signal, which has a length of m samples.

b. Set the desired number of reduced samples r and Y to be the matrix including N feature vectors from N different appliances (each column is a feature vector) ;

while $i \leq N$ **do**

1. Estimate the within-class-scatter (WCS) array Y_W as:

$$Y_W = \left(YDY - YWY^T\right) = YL_1Y^T \tag{15}$$

where $L_1 = D - W$ represents the Laplacian. W is a symmetric array that encompasses the WCS patterns and D constitutes a diagonal array in which its inputs represent the column sums of W (or row sums because W is symmetric);

2. Estimate the between-class-scatter (BCS) array Y_B as:

$$Y_B = (MEM^T - MBM^T) = ML_2M^T \tag{16}$$

where M is the mean matrix of total patterns. $L_2 = E - B$, B is a symmetric array that includes the BCS patterns, and E represents a diagonal array, its inputs are column/row sums of B;

3. Estimate the transformation matrix $\mathbf{H}_{FNPA-QR}$ as follows

$$\mathbf{H}_{FNPA-QR} = \arg \mathbf{maxtrace}\left(\frac{\mathbf{H}^T Y_B \mathbf{H}}{\mathbf{H}^T Y_W \mathbf{H}}\right) \tag{17}$$

4. Apply the QR-decomposition to calculate the new transformation matrix Q, in which $H = Q \times R$, where R represents an upper-triangular array and Q defines an orthogonal array that satisfies $QQ^T = I$, where I is an identity matrix.

5. Make $\mathbf{H}_{FNPA-QR} = Q$ and project the feature matrix with the transformation matrix as follows:

$$Y_i' = \mathbf{H}_{FNPA-QR} \times Y_i \tag{18}$$

where the initial feature vector Y_i has m samples, the reduced vector feature Y_i' has r samples and $H_{FNPA-QR}$ is a matrix with a size of $m \times r$.

end

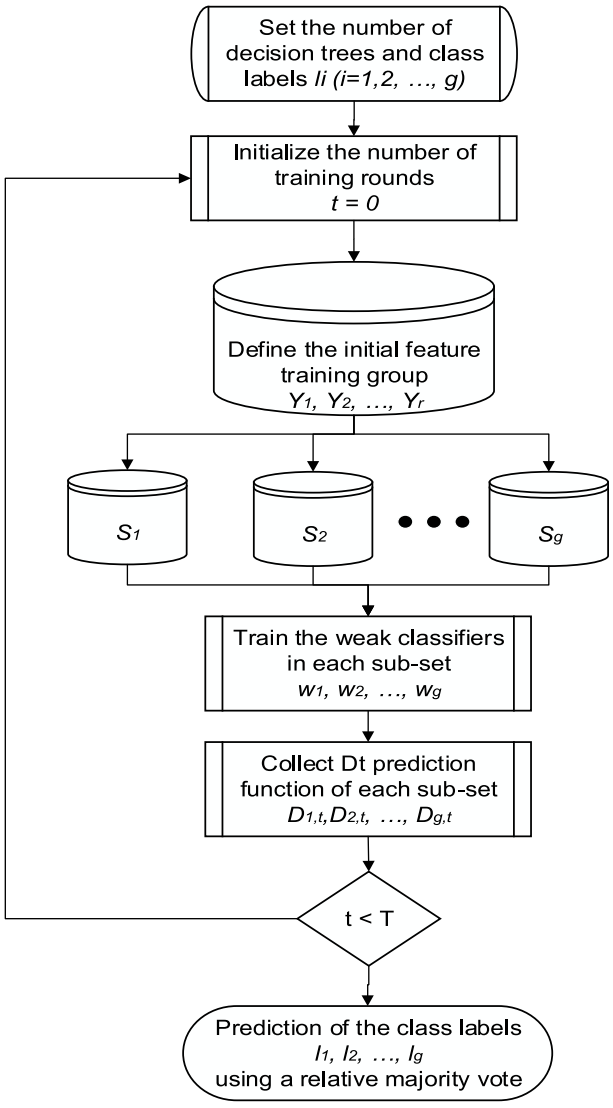

Fig. 4. Flowchart of the DBT algorithm used to identify appliances.

analysis (FLDA) [68]. The latter has been used to study the class relationship between samples, however the main drawback of FLDA is related to the fact that it could not find out the regional geometric structure of samples. Accordingly, in discriminant analysis, the regional arrangement is more prominent in comparison to the global one [69–71]. In addition, the discrimination ability between samples pertaining to different groups can be improved if the local structure is preserved.

To that end, the FNPA-QR introduces a novel feature projection scheme that can map the samples into a new subspace through analyzing neighboring samples. Consequently, it makes adjacent samples with the same label more close and in contrast, turns the adjacent patterns with different labels to be far away. In this regard, FNPA-QR keeps the contribution of data points to different classes. Algorithm 1 summarizes the main steps used to implement the FNPA-QR algorithm. Eq. (15) points out that Y_W aims at minimizing the gap among samples of the same group when projecting them, and thereby it can preserve the neighborhood.

3.5. Decision Bagging Tree (DBT) classifier

The DBT model is a powerful classifier that did not receive its merit in practice. The importance of DBT comes from the fact that it can achieve a high classification performance by using a fusion of various weak classifiers. Specifically, this model builds upon an idea of combining multiple weak classifiers in order to develop a strong model. Put differently, these weak classifiers complement one another to improve the classification performance. Further, based on a recent work described in [12], in which the DBT algorithm is tested for another application that focuses on the detection of anomalous power consumption, this model has been very successful and has outperformed other classification models.

Fig. 4 explains in detail the steps required to implement the DBT classifier. If we consider a training set $Y = Y_1, Y_2, \ldots, Y_r$ that refers to the feature vector of an appliance extracted using FNPA-QR and let assume the total number of rounds is T. After initializing the training round $t = 0$, the initial training group is divided into g new sub-groups and then the weak classifiers are trained in each sub-group. Following, g decision tree prediction functions are collected $D_{1,t}, D_{2,t}, \ldots, D_{g,t}$. Moving forward, if $t \leq T$, the previous steps are repeated. Otherwise, the predictions of class labels $l_1, l_2, \ldots, l_g$ are generated using a majority vote process.

4. Experimental results

Different evaluation stages are performed in order to validate the proposed NILM system. In this section, we outline each stage separately starting by describing the properties of power consumption databases.

4.1. Datasets description

Before validating the proposed system, we briefly describe the characteristics of the databases investigated for the validation process:

- ACS-f2: is the second version of the appliance consumption signature repository. It encompasses the electricity consumption footprints of various electrical device categories using 0.1 Hz sampling frequency [58]. To validate the proposed NILM system, 11 appliance classes from the ACS-F2 are selected randomly and being used in this framework.
- REDD: Collects load usage footprints of six domestic buildings at a device-specific level and aggregated-level [60]. A sampling frequency of 0.33 Hz has been deployed for a period of 3–19 days to glean the energy usage fingerprints of various domestic appliances.
- WITHED: includes the power consumption signatures of the device start-ups collected from up to 110 electrical devices, categorizing up to 47 appliance groups. For each appliance category, a set of power consumption fingerprints is collected from different appliance manufacturers and all of them are gathered at a sampling rate of 44 kHz [59]. In this framework, we use 11 appliance categories to validate the proposed system.

The accuracy and F1 score metrics have been considered in this framework to evaluate the performance of the proposed method and guarantee an objective performance inspection, they are measured as follows [72]:

$$Accuracy = \frac{TP + TN}{TP + TN + FP + FN} \tag{19}$$

$$F1score = 2 \times \frac{precision \times recall}{precision + recall} \tag{20}$$

where $precision = \frac{TP}{TP+FP}$ and $recall = \frac{TP}{TP+FN}$. TP, TN, FP and FN depict the number of true positives, true negatives, false positives and false negatives, respectively.

4.2. Event detection

To demonstrate how the edge detector can effectively detect power events of individual appliances for the aggregated power consumption signal, Fig. 5 portrays an example of a main consumption collected from House 1 under REDD dataset for a whole day, in addition to various individual power event vectors. The latter is extracted from the main power consumption signal to represent a set of appliances defined as: oven, stove, washing dryer, kettle and vacuum cleaner. It is clearly seen that the power consumption of each appliance has a specific consumption form and power range. This helps in facilitating the task of the DBT classifier to identify device-specific events and effectively differentiate between the various appliances contributing to the main consumption. Moreover, each individual appliance event vector is portrayed in a way to have the same length as the aggregated signal, in which the transient cycle represents the most relevant information that distinguishes an appliance others.

Table 1
Performance of different descriptor combinations used to implement the FTDF scheme in terms of the accuracy and F1 score.

Descriptor	ACS-F2		REDD		WHITED	
Combination	Accuracy	F1 score	Accuracy	F1-score	Accuracy	F1 score
$S_{F1}, S_{F2}, S_{F3}, S_{F4}$	**99.41**	**98.93**	**100**	**100**	**100**	**100**
$S_{F2}, S_{F3}, S_{F4}, S_{F5}$	92.12	91.71	94.95	94.67	91.63	91.08
$S_{F3}, S_{F4}, S_{F5}, S_{F6}$	93.97	93.75	95.23	94.59	91.31	90.46
$S_{F4}, S_{F5}, S_{F6}, S_{F7}$	79.53	79.36	81.76	81.2	78.63	78.69
$S_{F1}, S_{F3}, S_{F5}, S_{F7}$	89.28	88.7	90.85	90.63	88.91	88.49

4.3. Performance of the fusion of TD features (FTDF)

With a view to evaluating the performance of the proposed FTDF, the obtained results in terms of the accuracy and F1 score are compared to those extracted from the various TD descriptors described in Section 3.3.1. A segmentation based on an overlapping rate of 1/4 the window size is utilized for all the descriptors during this study.

Fig. 6 portrays the comparison of the accuracy and F1 score performances of FTDF against the other TD feature extraction schemes, according to a window size ranging from 64–4096 for both the REDD and WHITED datasets and 4–256 for the ACS-F2. The obtained results witnessed the superiority of the proposed FTDF in the three cases, the best performance can be obtained for a window length of 3072 for both REDD and WHITED while for the ACS-F2 the best performance can be reached with a window length of 128. This can be justified by the fact that through aggregating several weak descriptors using the proposed fusion architecture, a powerful descriptor is designed that improves feature discrimination ability and thus optimizes the classification process. Therefore, this is the main advantage of the this fusion process. Furthermore, the slight difference between the results collected from the WHITED, REDD and the ACS-F2 is due to the fact that these datasets are quite different and use different sampling rate and further different signal length. The WHITED and ACS-F2 collect just the power consumption signatures of each device for a very short duration while the REDD gathers energy usage footprints of each appliance for the whole day.

In order to evaluate which descriptor fusion can provide the best performance in terms of the accuracy and F1 score, the results of different descriptor combinations have been assessed. In each combination, four descriptors divided into two couples are used, in which the correlation of each descriptor couple is measured, then the obtained correlations are fused, as discussed in Section 3-C2. Table 1 depicts the accuracy and F1 score obtained for five study cases. It is clearly seen that the combination ($S_{F1}, S_{F2}, S_{F3}, S_{F4}$) that refers to the fusion of the MADV, IAVF, RMSF and WLF descriptors provides the best performance. Specifically, up to 100% of both the accuracy and F1 score have been reported for the WHITED dataset, 99.79% accuracy and 99.76% F1 score have been achieved under the REDD database, and up to 99.41% accuracy and 98.93% F1 score have been reached under the dataset, respectively.

Fig. 7 presents a performance comparison of the proposed NILM system when different fusion strategies are considered. It is clearly evident that the multiplication strategy achieves better accuracy and F1 score under the three datasets of the case study. For example, under the REDD dataset and using the multiplication-based fusion, 3.94% accuracy and 4.57% F1 score gains have been achieved in comparison with the concatenation scheme, while up to 1.98% accuracy and 2.21% F1 score improvements have been attained versus the summation strategy.

4.4. Comparison with other dimensionality reduction

Under the dimensionality reduction stage, the performance of the presented appliance identification based FNPA-QR system is validated with reference to other feature projection schemes, including principal

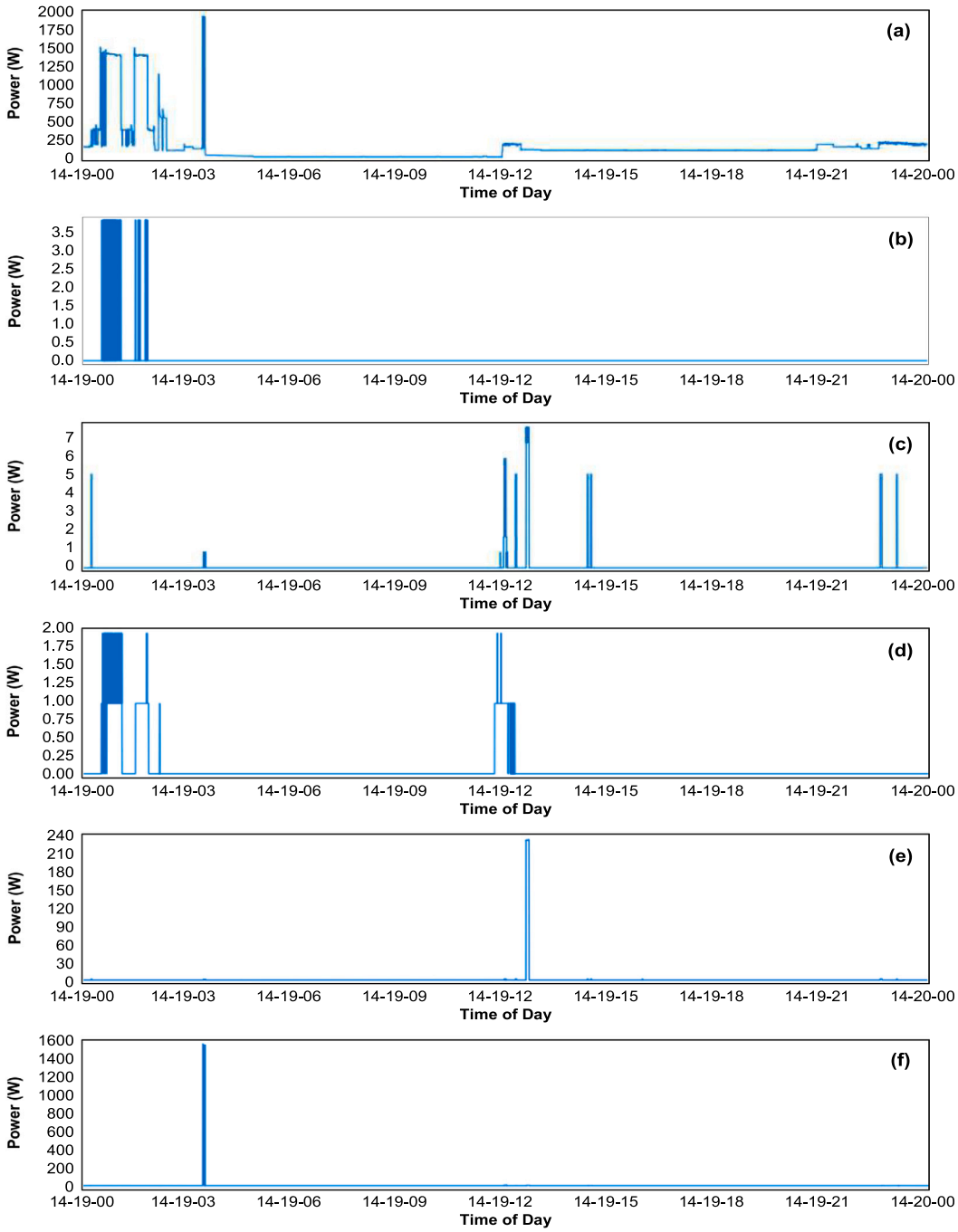

Fig. 5. Example of extracted power events of different individual appliances: (a) aggregated power, (b) oven, (c) stove, (d) washing dryer, (e) kettle and (f) vacuum cleaner.

component analysis (PCA) [73], linear discriminant analysis (LDA) [73] and FLDA [68]. Table 2 depicts the accuracy, F1 score and computational complexity of the proposed technique based on FNPA-QR in comparison to other dimensionality reduction approaches. The outputs are collected using Python 3.7 running on a laptop having a Core i7-85500 with 32 GB RAM and 1.97 GHz.

It is easily witnessed that by using the FNPA-QR the accuracy and F1 score are highly improved in comparison to other feature projection schemes. However, the time complexity is increased and this is due to the fact that FNPA-QR uses a fuzzy process along with the QR decomposition. Fortunately, considering the optimal outputs that have been realized by the proposed approach based FNPA-QR with reference to the accuracy and F1 score, the time complexity issue can be easily resolved by using powerful processors or optimizing the FNPA-QR algorithm.

4.5. Comparison with other classifiers

We perform a performance comparison of the DBT classifier versus other machine learning models, including support vector machines (SVM), K-nearest neighbors (KNN), decision trees (DT) and DNN, which operate by reference to different classification parameters and when the FTDF is considered as well. Table 3 illustrates the accuracy and F1 score outputs obtained for ACS-F2, REDD and WHITED datasets. A window length of 128 is considered for the ACS-F2 while for both REDD and WHITED, a window length of 3072 is reserved. It is clearly shown that the DBT outperformed the other classifiers with respect to the accuracy

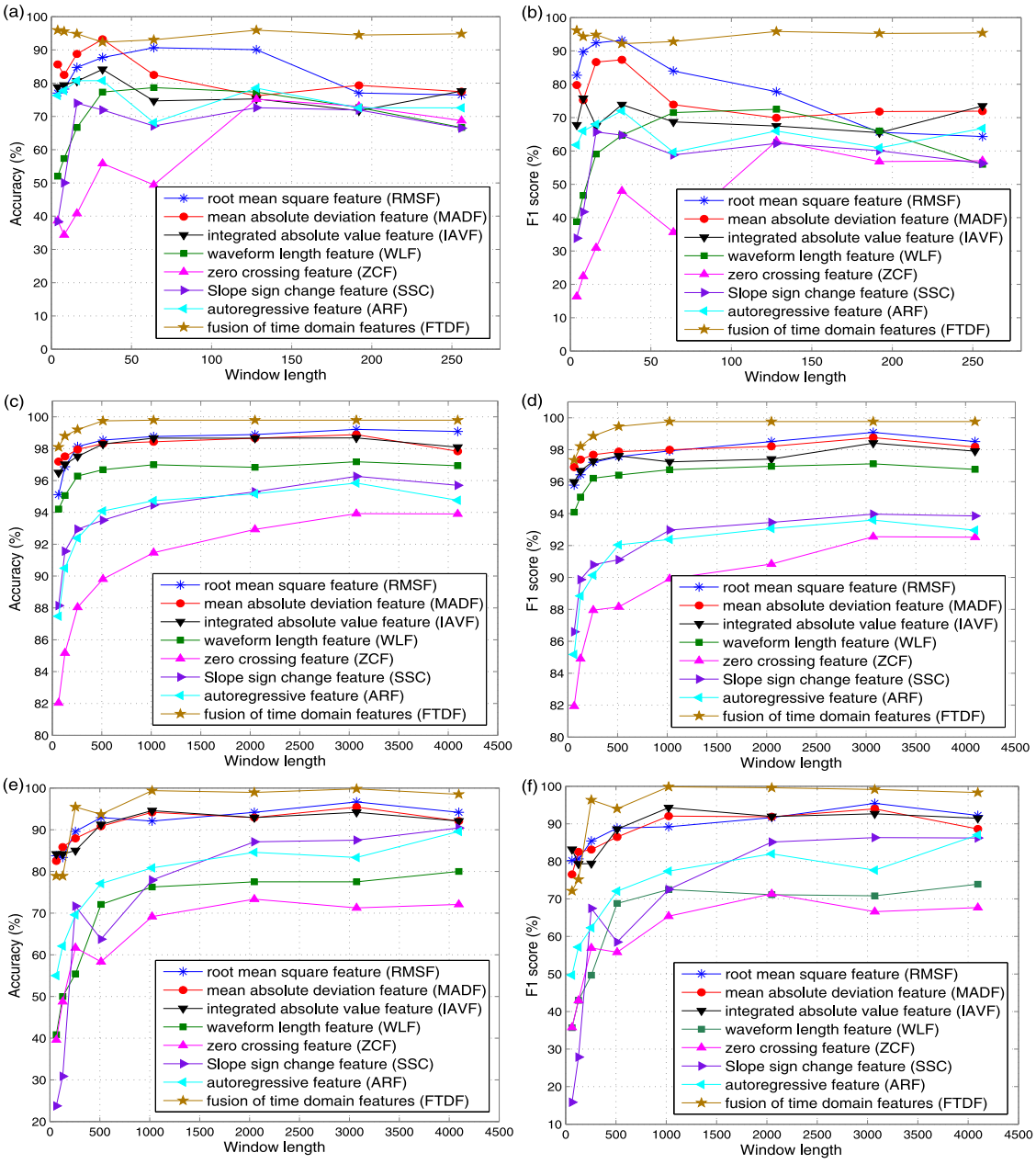

Fig. 6. Accuracy and F1 score variations according to the window length for; (a) and (b): the ACS-F2, (c) and (d): the REDD and (e) and (f): the WHITED, respectively.

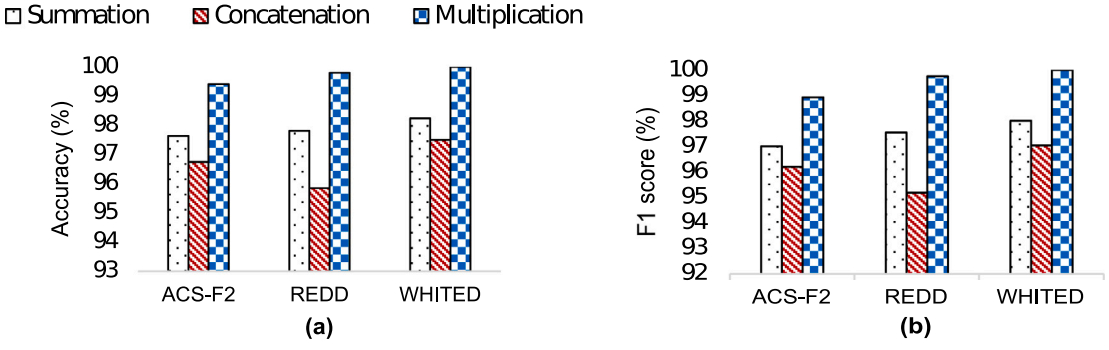

Fig. 7. Performance of the proposed solution using different fusion strategies in terms of: (a) accuracy and (b) F1 score.

Table 2
Performance of FNPA-QR versus other techniques in terms of the accuracy, F1 score and time complexity.

Dataset	Performance	PCA	LDA	FLDA	FNPA-QR
ACS-F2	Accuracy (%)	78.35	83.17	92.94	**99.41**
	F1 score (%)	76.61	82.49	92.71	**98.93**
	Time (s)	**0.0035**	1.81	0.71	0.85
REDD	Accuracy (%)	86.3	92.65	95.22	**99.79**
	F1 score (%)	85.78	92.42	94.86	**99.76**
	Time (s)	**0.09**	34.3	15.2	22.5
WHITED	Accuracy (%)	83.57	91.26	94.17	**100**
	F1 score (%)	83.29	90.76	93.9	**100**
	Time (s)	**0.021**	8.8	3.8	4.4

and F1 score. This superiority is related to the fact that by using multiple weak classifiers, the DBT develops a strong learning process leading to an accurate classification ability. Furthermore, the DBT has the same properties of being very speed and less time complexity demanding as the weak classifiers.

Moreover, the proposed solution based on the DBT classifier has been evaluated under three datasets with distinct sampling frequencies. This gives more credibility to our framework since it demonstrates that the proposed NILM architecture can work at any frequency range and its performance is not depending on the sampling frequency, in contrast to other NILM systems, in which their performance can significantly vary when the sampling frequency is varied from a level to another (through changing the dataset). As illustrated in Table 3, e.g. using SVM (Linear Kernel), the accuracy is 94.05%, 93.74% and 98.31% under the ACS-F2 (0.1 Hz), REDD (0.33 Hz) and WHITED (44 kHz) datasets, respectively. For the KNN (K = 10/Cosine dist), the F1 score rates are 94.43%, 96.5% and 87.93% under the ACS-F2, REDD and WHITED datasets, respectively. Consequently, it is worth mentioning that the performance highly varies when the frequency sampling has been changed.

4.6. Comparison with recent NILM systems

In this section, a comparison of the proposed system versus various recent NILM frameworks is conducted under the REDD dataset. Different, parameters are evaluated, including (i) the feature based class, (ii) the nature of the feature, (iii) the machine learning process, (iv) the number of appliance categories used in the validation process, (v) the achieved accuracy and F1 score. Table 4 summarizes the outcomes of the comparison study, in which it is clearly shown that the proposed solution outperforms the other techniques considered in this study.

Finally, it is worth noting that the empirical evaluations considered in this framework have provided us the opportunity to illustrate the various benefits of our algorithm in comparison with various existing techniques. For instance, using ACS-F2 and WHITED datasets to train the proposed approach can cover almost all existing domestic appliances usually used in households, and hence there is no need to train it again when it is applied to real-world applications. In the worst case, these datasets can easily be updated with new appliance signatures if there is a new appliance, which is not included in the training datasets. Furthermore, it is of significant importance to mention that the use of DBT in our solution has been selected because this kind of classifier does not require a large amount of data in the training step in comparison to other models, such as DNN, CNN and GAN. The latter require large-scale datasets and are usually computationally intensive and hard to implement on low-cost computing platforms. Thus, their application for non-intrusive load monitoring is not practical. While, for our solution, it is possible to train the DBT classifier with markedly less data that can easily be collected in a household.

Moreover, the proposed scheme provides several practical advantages, since it has been used in different scenarios. Considering three different datasets with distinct characteristics to evaluate the proposed solution was mainly planned to demonstrate its benefits. Therefore, the proposed scheme does not rely on only using the acquisition of consumption data of single electrical appliances because the proposed solution has been tested on both scenarios: first, in ACS-F2 and WHITED datasets the training is conducted using appliance-level signatures stored in these datasets before testing the proposed algorithm on aggregated data. Second, in REDD dataset aggregated consumption signals are used to train our algorithm after detecting the events and extracting the features. Accordingly, the proposed scheme provides promising results in both scenarios, which demonstrates that it can be applied easily in practical scenarios. In addition, these datasets have been gathered from different countries, i.e. REDD and ACS-F2 datasets have been collected in USA and Switzerland, respectively, while the WHITED dataset has been gleaned from several households located in different regions around the world. Therefore, this has helped in discussing the performance of proposed solution from the viewpoints of different countries.

4.7. Experimental validation

To evaluate the capability of implementing the proposed NILM solution for real applications, it has been implemented under (i) a laptop having a Core i7-85500 with 32 GB RAM and 1.97 GHz, and (ii) a Jetson TX1 platform that has an NVIDIA Maxwell GPU with 256 NVIDIA CUDA Cores and 16 GB [79]. Accordingly, the proposed algorithm has been implemented to extract device-specific data gathered in ACS-F2 and REDD datasets, respectively, using Python 3.7. Following, we have collected the computational costs and investigate the real-time capability of the our solution. Table 5 presents the performance obtained in terms of the training and test times on the laptop the Jetson TX1, where the multicore central processing unit (CPU) and graphics processing unit (GPU) are considered. First, it is worth noting that the computational times recorded on ACS-F2 are much lower than those achieved under REDD, this is mainly due to the fact that the appliance signatures is ACS-F2 have been collected for short time periods, while under REDD, they have been gleaned for the whole day

Table 3
Accuracy and F1 score of the proposed DBT model based FTDF and FNPA-QR compared to other classifiers.

ML	Classifier	ACS-F2		REDD		WHITED	
algo	parameters	Accuracy	F1 score	Accuracy	F1 score	Accuracy	F1 score
SVM	Linear Kernel	94.05	93.74	95.51	95.2	98.31	98.09
SVM	Quadratic kernel	92.22	91.57	93.48	93.03	90.83	86.17
SVM	Gaussian kernel	94.63	93.6	95.38	95.29	93.41	90.91
KNN	K = 1/Euclidean distance	97.24	97.19	98.06	98.05	96.49	93.73
KNN	K = 10/Weighted Euclidean dist	96.21	95.94	98.14	98.1	95.43	92.82
KNN	K = 10/Cosine dist	94.75	94.43	96.66	96.5	92.08	87.93
DT	Fine, 100 splits	98	97.69	99.1	99.04	93.87	91.98
DT	Medium, 20 splits	93.49	93.87	96.61	93.89	94.07	90.86
DT	Coarse, 4 splits	92.91	89.82	94.33	92.17	91.8	88.62
DNN	50 hidden layers	96.17	95.88	98.22	98.21	97.02	96.97
DBT	**30 learners, 42k splits**	**99.41**	**98.93**	**99.79**	**99.76**	**100**	**100**

Table 4
Comparison of the proposed solution with other recent NILM frameworks under REDD dataset in terms of: NILM class, feature, learning scheme, # appliance categories, accuracy and F1 score.

Work	NILM class	Feature	Learning scheme	# appliance categories	Accuracy (%)	F1 score
[74]	Sparse coding	Multi-Label Sparse Representation	Unsupervised	5	–	68.01
[75]	DNN	Recurrent neural network (RNN)	Supervised	8	95	62.87
[76]	Sparse coding	Ttransform learning formulation	Unsupervised	7	75.5	–
[50]	Graph signal processing	Graph-based filtering	Unsupervised	8	76.08	69
[77]	DNN	Autoassociative Neural Network	Supervised	5	98.7	95.3
[78]	Time/frequency analysis	Delta of the V–I trajectory	Supervised	10	95.23	96.43
Our	Time/frequency analysis	Fusion of TD descriptors	Supervised	8	**99.79**	**99.76**

Table 5
Computational time of the proposed NILM solution using the experimental validation.

ACS-F2						REDD					
Training			Testing			Training			Testing		
Laptop	Jetson TX1		Laptop	Jetson TX1		Laptop	Jetson TX1		Laptop	Jetson TX1	
	CPU	GPU		CPU	GPU		CPU	GPU		CPU	GPU
32.35	94.11	36.15	0.071	0.27	0.084	93.31	283.63	119.37	0.19	0.83	0.25

periods. Second, it has been clearly shown that the laptop has the best performance for both ACS-F2 and REDD datasets. In addition, the Jetson TX1 with GPU has also achieved low computational costs, which have markedly been inferior than those of the Jetson TX1 with CPU. Overall, these results prove that the proposed NILM solution could be implemented in real-time applications because less than 1 s is required to identify appliance-level consumption data for both the laptop and Jetson TX1.

5. Conclusion

This article presented a promising non-intrusive load monitoring method for capturing appliance-level consumption patterns enjoying affordable, easy implementation, and potential scalable commercialization. The performance analysis of the proposed non-intrusive load monitoring system with the ACS-F2, REDD and WHITED datasets gathered at 0.1 Hz, 1 Hz and 44 kHz, respectively, are considered in this framework. The results of the evaluation study were encouraging with accuracies ranging from 99.41% for the ACS-F2 to 100% for both the REDD and WHITED databases. Moreover, the superiority of the proposed fuzzy-neighbors preserving analysis based QR-decomposition scheme was also demonstrated by comparing their performance to other dimensionality reduction techniques even if it slightly increased the computational time.

From the hardware implementation perspective, it has been demonstrated that our solution could be implemented on different computing devices, e.g. a laptop or a multi-core embedded platform, and the computational cost is mainly related to the length of the power consumption signatures. Considering the case of ACS-F2 dataset, the computational cost of the proposed non-intrusive load monitoring system was relatively low because the power consumption signatures of appliances have been recorded for short time periods. However, for the case of REDD dataset, the computational time has comparatively been increased. This was mainly due to the fact that in REDD dataset, each appliance consumption footprint has been gleaned for a one-day period. All in all, a real-time application could be supported ob both a laptop or a multi-core computing device since less than 1 s is required to identify individual appliances.

Finally, it is worth noting that our future work will be devoted to developing (i) an energy-efficiency recommender system that analyzes specific appliance consumption patterns collected using the proposed NILM approach, and (ii) a smartphone application to provide end-users with convincing, habit-transforming energy-saving recommendations and visualizations.

CRediT authorship contribution statement

Yassine Himeur: Conception and design of study, Acquisition of data, Analysis and/or interpretation of data, Writing - original draft. **Abdullah Alsalemi:** Conception and design of study, Acquisition of data, Analysis and/or interpretation of data, Writing - original draft. **Faycal Bensaali:** Conception and design of study, Analysis and/or interpretation of data, Writing - original draft, Writing - review & editing. **Abbes Amira:** Conception and design of study, Analysis and/or interpretation of data, Writing - original draft, Writing - review & editing.

Declaration of competing interest

The authors declare that they have no known competing financial interests or personal relationships that could have appeared to influence the work reported in this paper.

Acknowledgments

This paper was made possible by National Priorities Research Program (NPRP) grant No. 10-0130-170288 from the Qatar National Research Fund (a member of Qatar Foundation). The statements made herein are solely the responsibility of the authors. All authors approved the version of the manuscript to be published.
Open Access funding provided by the Qatar National Library.

References

[1] Das A, Annaqeeb MK, Azar E, Novakovic V, Kjaergaard MB. Occupant-centric miscellaneous electric loads prediction in buildings using state-of-the-art deep learning methods. Appl Energy 2020;269:115135.
[2] Himeur Y, Alsalemi A, Al-Kababji A, Bensaali F, Amira A. Data fusion strategies for energy efficiency in buildings: Overview, challenges and novel orientations. Inf Fusion 2020;64:99–120.
[3] He K, Stankovic L, Liao J, Stankovic V. Non-intrusive load disaggregation using graph signal processing. IEEE Trans Smart Grid 2018;9(3):1739–47.
[4] Zhou Y, Shi Z, Shi Z, Gao Q, Wu L. Disaggregating power consumption of commercial buildings based on the finite mixture model. Appl Energy 2019;243:35–46.
[5] Cominola A, Giuliani M, Piga D, Castelletti A, Rizzoli A. A hybrid signature-based iterative disaggregation algorithm for non-intrusive load monitoring. Appl Energy 2017;185:331–44.
[6] Wei Y, Xia L, Pan S, Wu J, Zhang X, Han M, Zhang W, Xie J, Li Q. Prediction of occupancy level and energy consumption in office building using blind system identification and neural networks. Appl Energy 2019;240:276–94.
[7] Alsalemi A, Himeur Y, Bensaali F, Amira A, Sardianos C, Varlamis I, Dimitrakopoulos G. Achieving domestic energy efficiency using micro-moments and intelligent recommendations. IEEE Access 2020;8:15047–55.

[8] Li D, Dick S. Residential household non-intrusive load monitoring via graph-based multi-label semi-supervised learning. IEEE Trans Smart Grid 2019;10(4):4615–27.

[9] Safarzadeh S, Rasti-Barzoki M. A game theoretic approach for assessing residential energy-efficiency program considering rebound, consumer behavior, and government policies. Appl Energy 2019;233–234:44–61.

[10] Alsalemi A, Sardianos C, Bensaali F, Varlamis I, Amira A, Dimitrakopoulos G. The role of micro-moments: A survey of habitual behavior change and recommender systems for energy saving. IEEE Syst J 2019;13(3):3376–87.

[11] Devlin MA, Hayes BP. Non-intrusive load monitoring and classification of activities of daily living using residential smart meter data. IEEE Trans Consum Electron 2019;65(3):339–48.

[12] Alsalemi A, Ramadan M, Bensaali F, Amira A, Sardianos C, Varlamis I, Dimitrakopoulos G. Endorsing domestic energy saving behavior using micro-moment classification. Appl Energy 2019;250:1302–11.

[13] Himeur Y, Alsalemi A, Bensaali F, Amira A, Sardianos C, Varlamis I, Dimitrakopoulos G. On the applicability of 2d local binary patterns for identifying electrical appliances in non-intrusive load monitoring. In: Arai K, Kapoor S, Bhatia R, editors. Intelligent systems and applications. Cham: Springer International Publishing; 2021, p. 188–205.

[14] Zhao B, Ye M, Stankovic L, Stankovic V. Non-intrusive load disaggregation solutions for very low-rate smart meter data. Appl Energy 2020;268:114949.

[15] Welikala S, Dinesh C, Ekanayake MPB, Godaliyadda RI, Ekanayake J. Incorporating appliance usage patterns for non-intrusive load monitoring and load forecasting. IEEE Trans Smart Grid 2019;10(1):448–61.

[16] Rashid H, Singh P, Stankovic V, Stankovic L. Can non-intrusive load monitoring be used for identifying an appliance's anomalous behaviour?. Appl Energy 2019;238:796–805.

[17] Welikala S, Thelasingha N, Akram M, Ekanayake PB, Godaliyadda RI, Ekanayake JB. Implementation of a robust real-time non-intrusive load monitoring solution. Appl Energy 2019;238:1519–29.

[18] Piscitelli MS, Brandi S, Capozzoli A. Recognition and classification of typical load profiles in buildings with non-intrusive learning approach. Appl Energy 2019;255:113727.

[19] Sadeghianpourhamami N, Ruyssinck J, Deschrijver D, Dhaene T, Develder C. Comprehensive feature selection for appliance classification in NILM. Energy Build 2017;151:98–106.

[20] Liu B, Luan W, Yu Y. Dynamic time warping based non-intrusive load transient identification. Appl Energy 2017;195:634–45.

[21] Welikala S, Thelasingha N, Akram M, Ekanayake PB, Godaliyadda RI, Ekanayake JB. Implementation of a robust real-time non-intrusive load monitoring solution. Appl Energy 2019;238:1519–29.

[22] Chang H, Lee M, Lee W, Chien C, Chen N. Feature extraction-based hellinger distance algorithm for nonintrusive aging load identification in residential buildings. IEEE Trans Ind Appl 2016;52(3):2031–9.

[23] Hart GW. Nonintrusive appliance load monitoring. Proc IEEE 1992;80(12):1870–91.

[24] Cole AI, Albicki A. Data extraction for effective non-intrusive identification of residential power loads. In *Proceedings of the IEEE instrumentation and measurement technology conference (IMTC), Vol. 2* 1998, p. 812–5.

[25] Bonfigli R, Principi E, Fagiani M, Severini M, Squartini S, Piazza F. Non-intrusive load monitoring by using active and reactive power in additive factorial hidden Markov models. Appl Energy 2017;208:1590–607.

[26] Kong S, Kim Y, Ko R, Joo S. Home appliance load disaggregation using cepstrum-smoothing-based method. IEEE Trans Consum Electron 2015;61(1):24–30.

[27] Chang H-H. Non-intrusive fault identification of power distribution systems in intelligent buildings based on power-spectrum-based wavelet transform. Energy Build 2016;127:930–41.

[28] Himeur Y, Alsalemi A, Bensaali F, Amira A. Robust event-based non-intrusive appliance recognition using multi-scale wavelet packet tree and ensemble bagging tree. Appl Energy 2020;267:114877.

[29] Jimenez Y, Duarte C, Petit J, Carrillo G. Feature extraction for nonintrusive load monitoring based on s-transform. In: 2014 Clemson university power systems conference. 2014, p. 1–5.

[30] Liu C, Akintayo A, Jiang Z, Henze GP, Sarkar S. Multivariate exploration of non-intrusive load monitoring via spatiotemporal pattern network. Appl Energy 2018;211:1106–22.

[31] Lam HY, Fung GSK, Lee WK. A novel method to construct taxonomy electrical appliances based on load signaturesof. IEEE Trans Consum Electron 2007;53(2):653–60.

[32] Baets LD, Ruyssinck J, Develder C, Dhaene T, Deschrijver D. Appliance classification using VI trajectories and convolutional neural networks. Energy Build 2018;158:32–6.

[33] Liang J, Ng SKK, Kendall G, Cheng JWM. Load signature stud–part i: Basic concept, structure, and methodology. IEEE Trans Power Deliv 2010;25(2):551–60.

[34] Hassan T, Javed F, Arshad N. An empirical investigation of v-i trajectory based load signatures for non-intrusive load monitoring. IEEE Trans Smart Grid 2014;5(2):870–8.

[35] Bouhouras AS, Gkaidatzis PA, Panagiotou E, Poulakis N, Christoforidis GC. A NILM algorithm with enhanced disaggregation scheme under harmonic current vectors. Energy Build 2019;183:392–407.

[36] Cole A, Albicki A. Nonintrusive identification of electrical loads in a three-phase environment based on harmonic content. In *Proceedings of the 17th IEEE instrumentation and measurement technology conference (IMTC), Vol. 1*, 2000, p. 24–9.

[37] Srinivasan D, Ng WS, Liew AC. Neural-network-based signature recognition for harmonic source identification. IEEE Trans Power Deliv 2006;21(1):398–405.

[38] Shaw SR, Leeb SB, Norford LK, Cox RW. Nonintrusive load monitoring and diagnostics in power systems. IEEE Trans Instrum Meas 2008;57(7):1445–54.

[39] Wu X, Han X, Liu L, Qi B. A load identification algorithm of frequency domain filtering under current underdetermined separation. IEEE Access 2018;6:37094–107.

[40] Cominola A, Giuliani M, Piga D, Castelletti A, Rizzoli A. A hybrid signature-based iterative disaggregation algorithm for non-intrusive load monitoring. Appl Energy 2017;185:331.

[41] Gulati M, Ram SS, Singh A. An in depth study into using EMI signatures for appliance identification. In: Proceedings of the 1st ACM conference on embedded systems for energy-efficient buildings. BuildSys '14, New York, NY, USA: ACM; 2014, p. 70–9.

[42] Guedes JDS, Ferreira DD, Barbosa BHG, Duque CA, Cerqueira AS. Non-intrusive appliance load identification based on higher-order statistics. IEEE Lat Amer Trans 2015;13:3343–9.

[43] Parson O, Ghosh S, Weal M, Rogers A. An unsupervised training method for non-intrusive appliance load monitoring. Artificial Intelligence 2014;217:1–19.

[44] Makonin S, Popowich F, Bajic IV, Gill B, Bartram L. Exploiting HMM sparsity to perform online real-time nonintrusive load monitoring. IEEE Trans Smart Grid 2016;7(6):2575–85.

[45] Raiker GA, Reddy SB, Umanand L, Yadav A, Shaikh MM. Approach to non-intrusive load monitoring using factorial hidden Markov model. In: 2018 IEEE 13th international conference on industrial and information systems (ICIIS). 2018, p. 381–6.

[46] Kong W, Dong ZY, Hill DJ, Luo F, Xu Y. Improving nonintrusive load monitoring efficiency via a hybrid programing method. IEEE Trans Ind Inf 2016;12(6):2148–57.

[47] He K, Stankovic L, Liao J, Stankovic V. Non-intrusive load disaggregation using graph signal processing. IEEE Trans Smart Grid 2018;9(3):1739–47.

[48] Ortega A, Frossard P, Kovacevic J, Moura JMF, Vandergheynst P. Graph signal processing: Overview, challenges, and applications. Proc IEEE 2018;106(5):808–28.

[49] Stanković L, Daković M, Sejdić E. Introduction to graph signal processing. In: Stanković L, Sejdić E, editors. Vertex-frequency analysis of graph signals. Cham: Springer International Publishing; 2019, p. 3–108.

[50] Zhao B, He K, Stankovic L, Stankovic V. Improving event-based non-intrusive load monitoring using graph signal processing. IEEE Access 2018;6:53944–59.

[51] Qi B, Liu L, Wu X. Low-rate non-intrusive load disaggregation with graph shift quadratic form constraint. Appl Sci 2018;8(4):1–17.

[52] Zhai M-Y. A new graph learning-based signal processing approach for non-intrusive load disaggregation with active power measurements. Neural Comput Appl 2019;35:5495–504.

[53] Kolter JZ, Batra S, Ng AY. Energy disaggregation via discriminative sparse coding. In: Proceedings of the 23rd international conference on neural information processing systems - Volume 1. NIPS'10, USA: Curran Associates Inc.; 2010, p. 1153–61.

[54] Singh S, Majumdar A. Deep sparse coding for non-intrusive load monitoring. IEEE Trans Smart Grid 2018;9(5):4669–78.

[55] Wang B, Chen Z, Boedihardjo A, Lu C-T. Virtual metering: An efficient water disaggregation algorithm via nonintrusive load monitoring. ACM Trans Intell Syst Technol (TIST) 2018;9:1–30.

[56] Gupta M, Majumdar A. Robust supervised sparse coding for non-intrusive load monitoring. In: 2018 international joint conference on neural networks (IJCNN). 2018, p. 1–6.

[57] Nalmpantis C, Vrakas D. Machine learning approaches for non-intrusive load monitoring: from qualitative to quantitative comparation. Artif Intell Rev 2019;52(1):217–43.

[58] Ridi A, Gisler C, Hennebert J. ACS-F2 – A new database of appliance consumption signatures. In: 2014 6th international conference of soft computing and pattern recognition (SoCPaR). 2014, p. 145–50.

[59] Kahl M, Haq AU, Kriechbaumer T, Jacobsen H-A. WHITED-a worldwide household and industry transient energy data set. In: 3rd international workshop on non-intrusive load monitoring. 2016.

[60] Kolter JZ. REDD : A public data set for energy disaggregation research. In: Procededings of the 1st KDD workshop on data mining applications in sustainability (SustKDD). San Diego, CA, USA: ACM; 2011.

[61] Paradiso F, Paganelli F, Giuli D, Capobianco S. Context-based energy disaggregation in smart homes. Future Internet 2016;8:4.

[62] Batra N, Kukunuri R, Pandey A, Malakar R, Kumar R, Krystalakos O, Zhong M, Meira P, Parson O. A demonstration of reproducible state-of-the-art energy disaggregation using NILMTK. In: Proceedings of the 6th ACM international conference on systems for energy-efficient buildings, cities, and transportation. BuildSys '19, New York, NY, USA: Association for Computing Machinery; 2019, p. 358–9.

[63] Batra N, Kelly J, Parson O, Dutta H, Knottenbelt W, Rogers A, Singh A, Srivastava M. NILMTK: An open source toolkit for non-intrusive load monitoring. In: Proceedings of the 5th international conference on future energy systems. e-Energy '14, New York, NY, USA: Association for Computing Machinery; 2014, p. 265–76.

[64] Lotte F. A new feature and associated optimal spatial filter for EEG signal classification: Waveform Length. In *Proceedings of the 21st international conference on pattern recognition (ICPR2012)*, 2012, p. 1302–5.

[65] Godiyal AK, Verma V, Khanna N, Joshi D. Force myography and its application to human locomotion. In: Naik G, editor. Biomedical signal processing: advances in theory, algorithms and applications. Singapore: Springer Singapore; 2020, p. 49–70.

[66] Chen Q, Wu X, Liu T, Li H. Zero-crossing feature extraction based on threshold optimization for rolling element bearing. In: Zhu Q, Na J, Wu X, editors. Innovative techniques and applications of modelling, identification and control: selected and expanded reports from ICMIC'17. Singapore: Springer Singapore; 2018, p. 409–25.

[67] Bhattacharya A, Sarkar A, Basak P. Time domain multi-feature extraction and classification of human hand movements using surface EMG. In: 2017 4th international conference on advanced computing and communication systems (ICACCS). 2017, p. 1–5.

[68] Watada J, Tanaka H, Asai K. Fuzzy discriminant analysis in fuzzy groups. Fuzzy Sets and Systems 1986;19(3):261–71.

[69] Cai D, He X, Zhou K, Han J, Bao H. Locality sensitive discriminant analysis. In: Proceedings of the 20th international joint conference on artifical intelligence. IJCAI'07, San Francisco, CA, USA: Morgan Kaufmann Publishers Inc.; 2007, p. 708–13.

[70] Huang Y, Tang K, Sun Z. Locality sensitive discriminant analysis for classification of hyperspectral data. In: 2014 7th international congress on image and signal processing. 2014, p. 292–6.

[71] Gao Q, Liu J, Cui K, Zhang H, Wang X. Stable locality sensitive discriminant analysis for image recognition. Neural Netw 2014;54:49–56.

[72] Machlev R, Levron Y, Beck Y. Modified cross-entropy method for classification of events in nilm systems. IEEE Trans Smart Grid 2019;10(5):4962–73.

[73] Ramlee R, Muda AK, Syed Ahmad SS. PCA And LDA as dimension reduction for individuality of handwriting in writer verification. In: 2013 13th international conference on intellient systems design and applications. 2013, p. 104–8.

[74] Singh S, Majumdar A. Non-intrusive load monitoring via multi-label sparse representation-based classification. IEEE Trans Smart Grid 2020;11(2):1799–801.

[75] Linh NV, Arboleya P. Deep learning application to non-intrusive load monitoring. In: 2019 IEEE Milan powertech. 2019, p. 1–5.

[76] Gaur M, Majumdar A. Disaggregating transform learning for non-intrusive load monitoring. IEEE Access 2018;PP:1.

[77] Morais LR, Castro ARG. Competitive autoassociative neural networks for electrical appliance identification for non-intrusive load monitoring. IEEE Access 2019;7:111746–55.

[78] Wang AL, Chen BX, Wang CG, Hua D. Non-intrusive load monitoring algorithm based on features of V-I trajectory. Electr Power Syst Res 2018;157:134–44.

[79] Jetson tx1 developer kit. 2020, http://www.nvidia.com/object/jetson-TX1-dev-kit.htmll (Accessed: 2020-03-04).